European Journal of Immunology

HIV-TB co-infection impairs CD8$^+$ T-cell differentiation and function while dehydroepiandrosterone improves cytotoxic anti-tubercular immune responses

Guadalupe V. Suarez[1], Matías T. Angerami[1], María B. Vecchione[1], Natalia Laufer[1,2], Gabriela Turk[1], Maria J. Ruiz[1], Viviana Mesch[3], Bibiana Fabre[3], Patricia Maidana[3], Diego Ameri[2], Pedro Cahn[2,4], Omar Sued[4], Horacio Salomón[1], Oscar A. Bottasso[5] and María F. Quiroga[1].

[1]Instituto de Investigaciones Biomédicas en Retrovirus y SIDA, Universidad de Buenos Aires - CONICET, Argentina;

[2]Hospital Juan A. Fernández, Buenos Aires, Argentina;

[3]Departamento de Bioquímica Clínica, INFIBIOC, Facultad de Farmacia y Bioquímica, Universidad de Buenos Aires, Argentina;

[4]Área de Investigaciones Médicas, Fundación Huésped, Buenos Aires, Argentina;

[5]Instituto de Inmunología Clínica y Experimental de Rosario (IDICER), CONICET-UNR, Rosario, Santa Fe, Argentina.

Key words: TB; HIV; DHEA; co-infection; CD8$^+$ T cells; cell differentiation.

Correspondence and request of reprints: Guadalupe V. Suarez, MSc., Instituto de Investigaciones Biomédicas en Retrovirus y SIDA, University of Buenos Aires, Paraguay 2155 P.11, Capital Federal, C1121ABG, Buenos Aires, Argentina. Telephone (54) 11 4508-3689; fax (54) 11 4508-3705; email: suarez_guadalupe@hotmail.com

Received: 02-Feb-2015; Revised: 08-May-2015; Accepted: 01-Jun-2015.

This article has been accepted for publication and undergone full peer review but has not been through the copyediting, typesetting, pagination and proofreading process, which may lead to differences between this version and the Version of Record. Please cite this article as doi: 10.1002/eji.201545545.

DHEA: Dehydroepiandrosterone

HD: healthy donor

LTB: Latent tuberculosis infection

Mtb: *Mycobacterium tuberculosis*

TB: Tuberculosis

T_{CM}: Central Memory T cells

T_{EM}: Effector Memory T cells

T_N: naïve T cells

T_{TE}: Terminal Effector T cells

Abstract

Tuberculosis (TB) is the leading cause of death among HIV positive patients. The decreasing frequencies of terminal effector (T_{TE}) $CD8^+$T cells may increase reactivation risk in persons latently infected with *Mycobacterium tuberculosis (Mtb)*. We have previously shown that dehydroepiandrosterone (DHEA) increases the protective anti-tubercular immune responses in HIV-TB patients. Here, we aimed to study *Mtb*-specific cytotoxicity, IFN-γ secretion, memory status of $CD8^+$T cells, and their modulation by DHEA during HIV-TB co-infection. $CD8^+$T cells from HIV-TB patients showed a more differentiated phenotype with diminished naïve (T_N) and higher effector memory (T_{EM}) and terminal effector (T_{TE}) T-cell frequencies compared to healthy donors (HD) both in total and *Mtb*-specific $CD8^+$T cells. Notably, $CD8^+$T cells from HIV-TB patients displayed higher T_{TE} $CD45RA^{dim}$ proportions with lower CD45RA expression levels, suggesting a not-fully differentiated phenotype. Also, PD-1 expression levels on $CD8^+$T cells from HIV-TB patients increased although restricted to the $CD27^+$ population. Interestingly, DHEA plasma levels positively correlated with T_{TE} in $CD8^+$T cells and in vitro DHEA treatment enhanced *Mtb*-specific cytotoxic responses and terminal differentiation in $CD8^+$T cells from HIV-TB. Our data suggest that HIV-TB co-infection promotes a deficient $CD8^+$ T-cell differentiation, whereas DHEA may contribute to improving anti-tubercular immunity by enhancing $CD8^+$T-cell functions during HIV-TB co-infection.

Introduction

Nearly one third of the world's population is infected with *Mycobacterium tuberculosis* (*Mtb*), the etiologic agent of tuberculosis (TB). HIV co-infection is the main risk factor for progression from latent to active TB disease, increasing the risk of latent TB (LTB) reactivation up to 20-fold [1].

It is well established that $CD4^+$T cells are critical for resistance to *Mtb* [2]. *Mtb* infection also elicits $CD8^+$T-cell responses which are recruited to the lung during infection and found in the granulomas of infected people [3]. Although it is still unknown how $CD8^+$T cells may mediate protection against TB, it has been suggested that while $CD4^+$T cells are more important in controlling bacterial replication during the acute phase of infection, $CD8^+$T cells play a greater role during latency, possibly via immune-surveillance of cells with higher numbers of intracellular bacilli [4, 5]. Besides cytokine secretion (IFN-γ and TNF-α), $CD8^+$T cells can induce T-cell-mediated cytotoxicity of infected cells, the major function of these cells [6]. Also, cytotoxic $CD8^+$T cells are able to directly kill intracellular bacteria by releasing granule contents [7]. In fact, mice lacking perforin generally succumb to *Mtb* late during infection, consistent with the relevance of $CD8^+$T cells during chronic or LTB infection [8].

In line with this, TNF-α blockade, which increases TB reactivation considerably in LTB persons, decreases the frequency of *Mtb*-specific terminally differentiated (terminal effectors -T_{TE}-) $CD8^+$T cells, underscoring the potential role of this population with the highest cytotoxic potential among $CD8^+$T cells, in *Mtb* control [9, 10]. In this regard, while *Mtb*-specific $CD8^+$T cells in HIV^{neg}-LTB patients are mostly composed of T_{TE} cells ($CCR7^{neg}/CD45RA^+$), less differentiated Effector Memory T cells (T_{EM}, $CCR7^{neg}/CD45RA^{neg}$) predominate among *Mtb*-specific $CD8^+$T cells in HIV^{neg}-active TB patients [11]. Likewise, it has been recently found that cytokine-producing *Mtb*-specific $CD8^+$T cells from HIV-LTB, but not HIV-TB co-infected patients, also exhibited higher T_{TE} frequencies [12], suggesting a protecting role for $CD8^+$ T-cell terminal differentiation against TB. Also, in a preliminary

study, convalescing TB subjects with HIV co-infection exhibited a mild impairment in $CD8^+$ T-cell proliferation and IFN-γ production in response to *Mtb* antigens [13]. To our knowledge, no studies have yet been focused on *Mtb*-specific cytotoxic $CD8^+$ T-cell responses or their memory status on HIV-TB co-infected patients, which is central to understand the increasing susceptibility to TB in HIV infected patients given the proposed role of cytotoxic responses in LTB reactivation [9] and the importance of $CD8^+$ T-cell terminal differentiation in cytotoxic function [10].

Disease occurrence depends on a plethora of factors, including hormonal regulation of immune cells, which could shape infection outcome. Among hormonal effects on the immune response, glucocorticoids (GC) can promote a Th2 cytokine acquisition profile [14], facilitating Th2 activities, whereas its natural antagonist dehydroepiandrosterone (DHEA) is able to favor Th1 cytokine production and interfere with Th2 cytokine synthesis [15]. In fact, the synthetic DHEA derivative, 16 α-bromoepiandrosterone, exerts beneficial effects in clinical and experimental tuberculosis and in HIV patients [16-18]. We have previously demonstrated that in vitro treatment of PBMCs from HIV-TB patients with DHEA increased *Mtb*-specific IFN-γ responses and decreased FoxP3 expression in regulatory T cells, thus inducing a bias towards a protective anti-tubercular immune response [19].

Therefore, we aimed to study *Mtb*-specific cytotoxicity, IFN-γ secretion and effector / memory differentiation of $CD8^+$T cells during HIV-TB co-infection and their modulation by adrenal hormones, focusing on DHEA effects. Our data show that HIV-TB co-infection is associated with both impaired cytotoxic *Mtb*-specific $CD8^+$ T-cell responses and irregular $CD8^+$ T-cell differentiation, the latter evidenced by lower CD45RA expression levels in T_{TE} $CD8^+$T cells and higher PD1 expression restricted to $CD27^+$ $CD8^+$T cells. Additionally, in vitro DHEA treatment enhanced *Mtb*-specific $CD8^+$ T-cell cytotoxic responses and $CD8^+$ T-

cell terminal differentiation in HIV-TB. We propose that DHEA may contribute to improving anti-tubercular immunity by enhancing $CD8^+$ T-cell functions in HIV-TB patients.

Results

Functional subset distribution among peripheral $CD8^+$T cells in HIV-TB, HIV-LTB, HIV^+ and HD

In response to antigens, naïve $CD8^+$T cells (T_N) proliferate and differentiate into effector cells, which can be defined into at least three phenotypic groups according to their surface marker expression (reviewed in [10]). We analyzed bulk $CD8^+$ T-cell differentiation based on the expression of CD27 and CD45RA surface proteins as depicted in Figure 1 [20-23]. HIV-infected patients with active TB (HIV-TB) or latent TB (HIV-LTB) and HIV^+ patients with no *Mtb* co-infection (HIV) displayed different subset distributions in total peripheral $CD8^+$T cells compared to healthy donors (HD) (Figure 1A, pies). Moreover, both HIV-TB and HIV-LTB patients showed lower T_N but only HIV-TB patients showed higher T_{EM} and T_{TE} frequencies in total $CD8^+$T cells than HD (Fig. 1A, lower panel and B). Additionally, both HIV-TB and HIV-LTB patients exhibited a higher T_{TE}/T_N ratio compared to HD (Fig. 1C), thus indicating a shift to terminal differentiation among total $CD8^+$T cells in co-infected patients. These results are in line with the effect of *Mtb* infection on $CD8^+$ T-cell differentiation towards an effector phenotype proposed previously [11].

In order to establish whether the differences observed in circulating effector/memory subset proportions occurred due to alterations in the differentiation path, we evaluated transitions between effector/memory subsets by analyzing the correlation between phenotype proportions as described elsewhere [21, 24]. A statistically significant negative correlation between the proportions of two given subsets suggests that transitions between those populations are likely to occur. We observed a strong negative correlation between the

percentage of T_{TE} and T_{EM} in bulk $CD8^+$T cells from HIV-TB individuals but not from HD (Fig. 1D). Although we also detected a significant negative correlation between the $\%T_{TE}$ and $\%T_{CM}$ in both groups (data not shown), such data suggest the occurrence of a distinct differentiation pattern induced by *Mtb* and/or HIV on total $CD8^+$T cells in co-infected patients that may account for the increment observed in T_{TE} proportions.

Extrapulmonary TB is more frequent among HIV infected patients but the mechanisms of such increased incidence are not fully understood [25]. In order to better understand if the alterations observed in $CD8^+$ T-cell differentiation were related to TB localization or *Mtb* load, we stratified HIV-TB patients according to TB localization or smear test results (the latter associated with bacterial burden [11, 26]). However, we could not detect any differences in the proportions of bulk $CD8^+$ T-cell subsets among sub-groups (Fig.1E, left and middle panels). Interestingly, highly active antiretroviral therapy significantly changed effector/memory distribution in bulk $CD8^+$T cells ($p=0.0349$ by partial permutation test) by reducing T_{EM} and augmenting T_N populations (Fig. 1E, right panel). This indicates a partial recovery of $CD8^+$T-cell homeostasis after anti-HIV treatment. Overall, these data indicate that HIV-TB co-infection induces a bias to terminal differentiation in total $CD8^+$T cells.

Effector/memory subsets phenotype in total $CD8^+$T cells from HIV-TB, HIV-LTB, HIV^+ and HD individuals

The CD45RA isoform of CD45 facilitates sustained T-cell receptor (TCR) signaling more efficiently than smaller isoforms like CD45R0 which contribute to the cessation of the immune response [27]. We observed a significantly lower relative intensity of CD45RA in T_{TE} $CD8^+$T cells in HIV-TB patients than HD (Fig. 2A and C). Additionally, despite the increment in $CD45RA^{hi}$ T_{TE} cells found in HIV-TB patients, $CD45RA^{dim}$ T_{TE} $CD8^+$T cells were increased remarkably both in HIV-TB and HIV-LTB patients compared to HD (Fig. 2B and C). This lower expression of CD45RA in bulk

$CD8^+$ T_{TE} cells from HIV-*Mtb* co-infected patients may reduce responsiveness in these cells since CD45RA enhances TCR signaling [28, 29].

During HIV infection, PD-1 expression is a marker for abnormal naïve/memory distribution in T cells [30]. We observed an increment in PD1 expression on bulk $CD8^+$T cells among HIV-TB and HIV^+ patients compared to HD (Fig. 2D, left panel). Interestingly, PD-1 expression was mainly restricted to $CD27^+CD8^+$T cells in HIV-TB but not in HD (Fig. 2E). We also detected increased proportions of $CD27^{neg}CD8^+$T cells among HIV-TB compared to HD (Figure 2D, right panel). Finally, we observed a positive correlation between the proportion of $PD1^+$ cells in $CD27^+CD8^+$T cells and the percentage of CD45RAdim T_{TE} in $CD8^+$T cells (Fig. 2F). These results suggest an association between increased proportions of not fully differentiated $CD8^+$T cells (in terms of CD45RA expression) and elevated percentages of exhausted $CD27^+CD8^+$T cells in HIV-TB patients. A higher expression of PD-1 in the $CD27^+$ population and a positive correlation between PD-1 expression on $CD27^+CD8^+$T cells and $CD45RA^{dim}$ cells in T_{TE} could imply an arrest of exhausted cells on a less differentiated and poor functional phenotype as observed in HIV^+ patients [31].

To sum up, these results suggest an impaired differentiation occurring concomitantly with an increased exhaustion of $CD8^+$T cells, both associated to HIV-TB co-infection.

Effect of in vitro Mtb *stimulation on $CD8^+$T cells in HIV-TB subjects*

We first observed that *Mtb*-induced degranulation and IFN-γ secretion in $CD8^+$T cells from HIV^+, HIV-LTB or HIV-TB patients were not significantly different from media levels (Fig. 3A). In contrast, in vitro *Mtb*-stimulation augmented both functions of $CD8^+$T cells in BCG-vaccinated HD. This deficient *Mtb*-specific response in infected individuals did not occur due to a general impairment in $CD8^+$T cells reactivity since all the individuals tested responded to α-CD3/α-CD28 stimulation (Supporting Information Fig. 2).

In order to establish that *Mtb* in vitro stimulation induces terminal differentiation on total $CD8^+$T cells and whether this induction differs between HIV-TB patients and HD, we assessed effector/memory distribution before and after *Mtb*-stimulation in both groups. Although we did not observe any changes in overall efector/memory distribution after *Mtb*-stimulation in any of the groups (by partial permutation test, data not shown), we detected a slight but still significant increase in $CD8^+$ T_{TE} and T_{EM} populations and a reduction in T_N and T_{CM} populations in HD after Ag-stimulation (Supporting Information, Table 2). Conversely, *Mtb*-stimulation did not induce any changes in T_{CM} populations among bulk $CD8^+$T cells in HIV-TB patients, but as observed in HD, it increased T_{EM} and T_{TE} cells and decreased T_N proportions.

On the other hand, when analyzing *Mtb*-specific $CD8^+$T cells, different effector/memory distributions were observed between HD and HIV-TB for the three functions tested (Fig. 3B and C -pies-). In HIV-TB patients, CD107a/b^+ and IFN-γ^+ $CD8^+$T cells showed higher T_{EM} and T_{TE} cells respectively, while the three CD107a/b^+, IFN-γ^+ and bifunctional $CD8^+$T cells displayed lower T_N cells than HD (Fig. 3C, right panel). These results show that, as shown before for total $CD8^+$T cells, *Mtb*-specific $CD8^+$T cells in HIV-TB are biased to more differentiated stages independently of cell function.

Finally, correlation analyses were performed in order to ascertain transitions between populations in *Mtb*-specific CD8 T cells, as described above, revealing a significantly negative correlation between the proportions of T_{TE} and T_{CM} among CD107a/b^+ *Mtb*-specific $CD8^+$T cells in HIV-TB patients (Fig. 3D), which suggests a differentiation path from T_{CM} to T_{TE} in these cells. In contrast, $CD107^+$ $CD8^+$T cells from HD showed a significantly negative correlation between $\%T_{TE}$ and $\%T_N$ (Fig. 3D). Notably, IFN-γ-producing $CD8^+$T cells exhibited transitions from T_N to T_{TE} (Fig. 3D) in both groups. These observations indicate that effector/memory transitions in cytotoxic but not in IFN-γ secreting *Mtb*-specific $CD8^+$T cells are altered in HIV-TB patients.

Adrenal hormones and their interrelation with $CD8^+$T cells *subsets in HIV-TB*

We have previously shown that HIV-TB co-infection is associated to lower DHEA plasma levels and higher cortisol/DHEA ratios [19]. Here, we aimed at establishing that the imbalance in adrenal hormone levels observed in HIV-TB patients was related to alterations in the $CD8^+$T-cell compartment. Therefore, we observed a positive correlation between DHEA plasma levels and the proportion of T_{TE} cells (Fig. 4A) or T_{TE} $CD45RA^{hi}$ in bulk $CD8^+$T cells in HIV-TB patients but not in HIV^+, HIV-LTB (Fig. 4A) or HD (data not shown). Even though a lower number of subjects was analyzed in HIV and HIV-LTB groups, data trends suggest no association between DHEA plasma levels and $CD8^+$ T_{TE} or T_{TE} $CD45RA^{dim}$ proportions in these groups. This lack of association would be in accordance with our previous observation of preserved DHEA levels in these patient groups [19]. No significant correlations were observed between DHEA plasma levels and the percentages of *Mtb*-specific $CD8^+$T cells or their effector/memory subsets in any of the groups studied (data not shown). Noteworthy, a strong positive correlation between *Mtb*-induced CD107a/b expression and cortisol plasma levels was observed in HIV-TB (Fig. 4B, left) but not in HD (Fig. 4B, middle). Interestingly, we did not find a similar correlation between cortisol plasma levels and HIV-specific $CD8^+$T cells in HIV^+ individuals (Fig. 4B, right), which suggests a unique adrenal imbalance related to the inflammation accompanying concomitant TB and HIV infections.

When analyzing the in vitro effect of DHEA on *Mtb*-specific $CD8^+$ T-cell cytotoxicity and IFN-γ responses in HIV-TB patients, we observed that the increment induced by DHEA treatment over *Mtb* responses positively correlated with $CD4^+$ T-cell counts (data not shown). Consistent with this, in those HIV-TB individuals with $CD4^+$ cell counts above 100 cells/uL, DHEA significantly increased *Mtb*-specific CD107a/b^+, IFN-γ and bifunctional responses in

$CD8^+$T cells (Fig. 4C). We did not observe any effects of DHEA on $CD8^+$ T-cell responses in those individuals with $CD4^+$ cell counts below 100 cell/µl (data not shown). These results indicate that, as shown previously [19], DHEA exerts its enhancer effect depending on the immune status of the individuals.

Effect of DHEA on $CD8^+$T-cell *differentiation induced by* Mtb-*stimulation*

As the proportion of peripheral T_{TE} $CD8^+$T cells positively correlated with DHEA plasma levels in HIV-TB patients (Fig. 4A), we investigated the effect of DHEA addition over both effector/memory distribution and function of *Mtb*-stimulated $CD8^+$T cells. Even though DHEA treatment did not modify the overall effector/memory distribution of *Mtb*-specific $CD8^+$T cells (by partial permutation test, data not shown), in vitro DHEA treatment significantly increased T_{TE} $CD107a/b^+$ cells in *Mtb*-stimulated $CD8^+$T cells (Fig. 5A and B). We did not find any modulation on effector/memory subsets when analyzing IFN-γ-producing or bifunctional $CD8^+$T cells from HIV-TB individuals (Fig. 5A, middle and right panels, respectively). On the contrary, DHEA treatment did not modulate any subsets of *Mtb*-specific $CD8^+$T cells in HD (data not shown).

On the other hand, we analyzed the effect of in vitro DHEA treatment on the expression of transcription factors involved in $CD8^+$T-cell differentiation [32]. When co-administered with *Mtb,* DHEA treatment increased Tbet expression and Tbet/Eomesodermine (Eomes) ratio, both associated with terminal differentiation, in $CD8^+$ cells from HD (Fig. 5C and E, respectively). In contrast, *Mtb* stimulation alone increased Bcl-6 expression and reduced Blimp-1/Bcl-6 ratio (Fig. 5G and H, respectively), both associated with memory cell differentiation. Finally, DHEA also reverted the *Mtb*-induced decrease in Blimp-1/Bcl-6 ratio (Fig. 5H).

Overall, these findings suggest that DHEA may bias *Mtb*-induced $CD8^+$T-cell differentiation towards an effector phenotype, probably through the increment in Tbet/Eomes ratio.

Effect of DHEA on in vitro Mtb-*specific CD8$^+$T-cell responses*

It has been proposed that the IFN-γ secreted by CD8$^+$T cells could enhance their cytolitic potential through macrophage activation [33]. Therefore, we analyzed the possible relationship between lytic degranulation and IFN-γ production in CD8$^+$T cells. While no significant correlation was observed between the percentages of CD107a/b$^+$ and IFN-γ$^+$ in CD8$^+$T cells from HIV-TB patients after in vitro *Mtb*-stimulation (Fig. 6A), DHEA addition induced a positive correlation between both parameters (Fig. 6B). This positive correlation was similar to that observed when stimulating PBMCs from HIV-TB with Cytomegalovirus, Epstein-Barr, and Influenza virus control peptide pool (CEF, Fig. 6C) or when stimulating PBMCs from HD with *Mtb* (Fig. 6D). Of note, CEF pool elicits responses against pathogens that, unlike HIV and *Mtb,* were either cleared (influenza) or controlled (CMV and Epstein-Barr). These results suggest that DHEA may at least partially restore the functional response of *Mtb*-specific CD8$^+$T lymphocytes in the context of HIV infection.

Discussion

Increasing experimental evidence over the past years has shown the relevance of $CD8^+$T cells on the anti-tubercular immune response [33]. The reduction in the frequency of $CD8^+CCR7^{neg}CD45RA^+$ T_{TE} cells and their granulysin content induced by anti-TNF-α immune therapy, a treatment known to dramatically increase TB reactivation in LTB patients, unraveled a critical role for these cells in maintaining latency and anti-microbial activity in *Mtb*-infected patients [9]. In this regard, we observed a bias to a more differentiated phenotype in total $CD8^+$T cells in HIV-TB patients, probably in an attempt to develop a more efficient anti-tuberculous response. Also, contrary to HD, T_{TE} cells derived from both T_{EM} and T_{CM} populations in HIV-TB individuals (see Fig. 1C), which could contribute to the increased T_{TE} proportions observed in these patients. However, we observed lower levels of CD45RA on $CD8^+$T cells in HIV-TB patients –compared to HD– that may reflect a lower cell responsiveness, since an enhancing role for CD45RA in TCR signaling in multiple sclerosis and in the human cell line Jurkat has been described [27-29]. Similarly, HIV infection induces a maturation defect on HIV-specific T_{TE} cells which may represent an HIV-induced evasion mechanism [34].

It is widely accepted that PD-1 reflects T-cell exhaustion in the context of chronic infections like HIV and TB [30, 35]. Our results also demonstrate that PD-1 levels are increased among $CD27^+CD8^+$T cells in HIV-TB patients, providing new evidence pointing to an exhausted phenotype restricted to those cells that home to lymph nodes. These results are in line with the association of PD1 expression to a $Tbet^{low}/Eomes^{hi}$ Transtional Memory phenotype in $CD8^+$T cells from HIV^+ patients observed by Buggert *et al.* [31]. Strikingly, our observation of a positive correlation between PD-1 expression on $CD27^+CD8^+$T cells (a population that includes T_N, T_{CM} and Transitional Memory cells) and % $CD45RA^{dim}$ cells in T_{TE} points to an arrest of exhausted cells on less functional phenotypes as observed in HIV^+ patients [31].

Several authors have explored the dynamics of *Mtb*-specific $CD4^+$T cells but just a few studies have been focused on *Mtb*-specific $CD8^+$T cells. However, to our knowledge, only three studies described *Mtb*-specific $CD8^+$T cells in the context of HIV co-infection [12, 13, 36]. At present, this is the first report addressing *Mtb*-specific cytotoxic $CD8^+$ T-cell responses and their memory status in HIV-TB co-infected patients. In TB patients, Rozot *et al.* ascertained that *Mtb*-specific $CD8^+$T cells were mostly T_{EM} cells [11]. On the other hand, Caccamo *et al.* studied the phenotype of *Mtb*-specific $CD8^+$T cells by tetramer staining in TB patients, and observed a predominance of T_{CM} and lower T_{TE} $CD8^+$T cells, both of which were reverted after anti-TB therapy [37]. Lastly, Chiacchio *et al*. observed higher *Mtb*-specific T_{TE} $CD8^+$T cells in HIV-LTB individuals, but not in HIV-TB patients [12]. Contrary to those data, we detected elevated levels of T_{TE} and T_{EM} $CD8^+$T cells in *Mtb*-specific IFN-γ+ and CD107a/b^+ cells respectively in HIV-TB compared to HD. These differences may be linked to the use of distinct stimuli and/or markers to define *Mtb*-specific and memory/effector populations but it is likely that HIV infection and its related alterations in the immune system homeostasis induce changes in *Mtb*-specific $CD8^+$T-cell differentiation. We also found that *Mtb*-specific CD107a/b^+ $CD8^+$T cells were fueled by T_{CM} in HIV-TB, whereas in HD, they originated mainly from T_N. On the contrary, IFN-γ+ T_{TE} originated from T_N both in HIV-TB and HD. These analyses show for the first time not only maturation but also cell transition differences depending on cell function during HIV-TB co-infection. Endocrine hormones, and particularly adrenal hormones such as DHEA, are prone to modulate immune functions during HIV-TB co-infection as described previously by our group [19]. According to this, the present study shows that DHEA enhances $CD8^+$ T-cell responses and terminal differentiation (Fig. 4A and 5A) in HIV-TB co-infected individuals, suggesting a protective role for DHEA against mycobacteria in these patients. Even though DHEA can directly increase $CD8^+$ T-cell responses as shown by our in vitro experiments, we did not find any correlation between DHEA plasma levels and the % of *Mtb*-specific $CD8^+$T

cells. As the amount of DHEA in plasma and the intensity of the immune response to *Mtb* are determined by several factors (i.e. activation of hypothalamus-pituitary axis [14], TB burden [38] or HIV disease progression [25], among others), the association between DHEA plasma levels and *Mtb*-specific $CD8^+$T cells proportions in our cohort could be masked by these other factors.

Contrary to our expectations, we detected a positive correlation between cortisol plasma levels and CD107a/b$^+$ $CD8^+$T cells in HIV-TB individuals (Fig. 4B). We propose that *Mtb* infection may induce an increment in cortisol levels while concomitantly increasing *Mtb*-specific $CD8^+$ T-cell responses, driving to the observed association. These findings may be interpreted as an attempt of the endocrine system to modulate the inflammation induced by both infections.

In the present study, we observed that DHEA plasma levels positively correlated with T_{TE} and, importantly, $CD45RA^{hi}$ T_{TE} proportions in $CD8^+$T cells, and in vitro DHEA increased cytotoxic T_{TE} $CD8^+$T cells and diverted the $CD8^+$ cell transcriptional profile to a terminal effector one. Since macrophage activation by IFN-γ increases antigen presentation [39], one can expect a direct association between *Mtb*-specific IFN-γ and cytotoxic responses [40]. Our results show that, contrary to HD, the above mentioned association is impaired in HIV-TB patients and, more important, that in vitro DHEA treatment could restore the positive correlation between *Mtb*-specific degranulating and IFN-γ- producing $CD8^+$T cells in HIV-TB patients. The latter results point to an indirect effect of DHEA on $CD8^+$T cells through antigen-presenting cells. Accordingly, we previously observed that DHEA improved the production of IL-12 and the antigen-specific T-cell responses induced by *Mtb*-stimulated dendritic cells [41]. Also, during *Lysteria monocytogenes* infection, IL-12 represses Eomes and enhances T-bet in effector $CD8^+$T cells, while after the resolution of infection and abatement of IL-12 signaling, Eomes expression rises whereas T-bet expression declines in memory $CD8^+$T cells [42]. Therefore, the effect of DHEA on $CD8^+$T-cell differentiation and

IFN-γ and cytotoxic responses may be mediated by an enhancement on IL-12 production as shown previously [42].

To date, this is the first report showing an in-depth analysis of the $CD8^+$ T-cell memory/effector phenotype in HIV-TB co-infected patients and its modulation by DHEA, paving the way for delineating novel approaches for a better management of *Mtb* infection in people living with HIV.

Methods

Patients

The present study has a cross-sectional design. Patients were evaluated at Hospital J.A. Fernández, Buenos Aires (Table 1). Groups: HIV^+: tuberculin skin test negative, chronically $HIV\text{-}1^+$ infected patients as determined by ELISA and confirmatory Western Blot.; HIV-LTB: $HIV\text{-}1^+$ individuals with latent TB as determined by tuberculin skin test; HIV-TB: $HIV\text{-}1^+$ patients with active TB and less than one-week of anti-TB therapy and HD: healthy donors. Diagnosis of TB was based on the identification of acid-fast bacilli in sputum, a positive culture of tuberculosis bacilli and clinical and/or radiological data. All individuals were Bacillus Calmette-Guérin-vaccinated. None of the recruited individuals received DHEA or glucocorticoid treatment. Some HIV-1 infected individuals were on antiretroviral treatment following current guidelines [43]. The Ethics Committee from Fundación Huésped approved the current study. Written informed consent was documented from all study subjects.

Hormone assessment

EDTA-anticoagulated blood samples were drawn during morning hours. Plasma Cortisol was measured by automated electrochemiluminescence immunoassay (Roche Diagnostics GmbH) and DHEA by radioimmunoassay (IMMUNOTECH) following manufacturer's instructions.

Antigens

Pre-titrated Mycobacterium tuberculosis H37Rv, Gamma-Irradiated Whole Cells (NR-14819, BEI Resources, NIAID, NIH) was used at 10 µg/ml final concentration. Cytomegalovirus, Epstein-Barr, and Influenza virus control peptide pool (CEF) was obtained from the NIH AIDS Reagent Program, Division of AIDS, NIAID, NIH. Lyophilized peptides were dissolved in dimethyl sulfoxide (DMSO) at 20 µg/µl and stored at -20°C.

Culture conditions

PBMCs were isolated by density gradient centrifugation on Ficoll-Hypaque and cultured at $2x10^6$ cells/ml with *Mtb* (10 µg/ml), CEF (2 µg/ml) or anti-CD3 (10ng/ml) and anti-CD28 (1 µg/ml) antibodies in 48 well plates with RPMI medium (Sigma-Aldrich) supplemented with 10% fetal bovine serum (PAA), 2 mM L-glutamine (Gibco BRL), 100 U/ml penicillin (PAA) and 100 mg/ml streptomycin (Gibco BRL), in the presence or absence of DHEA (Sigma-Aldrich, 10^{-7} M). After 16 or 72 h, cells were harvested, stained and analyzed by flow cytometry or $CD8^+$ cells were isolated and lysed as described below.

Flow cytometry

PBMCs were stained for CD3, CD4, CD8, CD27, CD45RA and PD-1 expression using specific mAbs (Biolegend). In some experiments, cultured PBMC were surface stained for CD3, CD8, CD27 and CD45RA; concomitantly, intracellular cytokine staining was performed to determine IFN-γ production as described elswhere [44, 45] and CD107a/b expression was determined (20 µl/ml; BDBiosciences) to measure $CD8^+$T lymphocyte cytotoxic degranulation as described previously [46]. Negative control samples were incubated with irrelevant, isotype-matched mAbs in parallel with experimental samples. Dead cells were excluded by using Live/Dead® (Life Technologies) viability probe following manufacturer's instructions. Samples acquisition and analysis were carried out on a FACSCanto flow cytometer using the BD FACSDiva software (BDBiosciences).

Real-time PCR

$CD8^+$ cells were isolated by positive selection using CD8 magnetic beads (BDBiosciences), and then harvested in Trizol® Reagent (Invitrogen) following manufacturer's instructions. Afterwards, total RNA was quantified by 260 nm absorbance and cDNA was synthesized by MMLV retrotranscription (Invitrogen) following manufacturer's instructions. Real Time PCR was performed using CyberGreen Select (Invitrogen) in a 7500 Real-Time PCR (Applied Biosystems) to determine the relative expression of the genes depicted in Table 1 from Supplementary Information. Data analysis was performed using LinRegPCR software [47].

Statistical Analysis

Statistical analyses were conducted using GraphPad Prism 5 version 5.04. Comparisons between groups were evaluated by the Kruskall-Wallis analysis of variance followed by post hoc comparisons (Dunn's test) when applicable. Paired sample comparisons were performed using the non-parametric Wilcoxon matched pairs test. Correlations were determined using Spearman's rank test. Statistical analysis and display of multicomponent distributions were performed by partial permutation test using SPICE v5.1 (http://exon.niaid.nih.gov/spice/) [48]. p values below 0.05 were considered significant.

Acknowledgments

We thank the study subjects for their participation, Federico Remes Lenicov and Silvia de la Barrera for continuous support, Sergio Mazzini for revising the manuscript, Graciela Ben for assistance in recruiting the patients and Diego Gonzalez for assistance in hormone assessment.

This work was supported by Agencia Nacional de Promoción Científica y Tecnológica (PICT 2010-0656 and PICT 2012-0059 M.F.Q.), University of Buenos Aires (UBACyT 20020120200050BA M.F.Q) and Consejo Nacional de Investigaciones Científicas y Técnicas (CONICET, PIP 0010 M.F.Q.).

Conflict of Interest Disclosure:

The authors declare no commercial or financial conflict of interest.

References

1 **Getahun, H., Gunneberg, C., Granich, R. and Nunn, P.,** HIV infection-associated tuberculosis: the epidemiology and the response. *Clin Infect Dis* 2010. **50 Suppl 3**: S201-207.

2 **Kaufmann, S. H., Cole, S. T., Mizrahi, V., Rubin, E. and Nathan, C.,** Mycobacterium tuberculosis and the host response. *J Exp Med* 2005. **201**: 1693-1697.

3 **Rahman, S., Gudetta, B., Fink, J., Granath, A., Ashenafi, S., Aseffa, A., Derbew, M.*et al.*,** Compartmentalization of immune responses in human tuberculosis: few CD8+ effector T cells but elevated levels of FoxP3+ regulatory t cells in the granulomatous lesions. *Am J Pathol* 2009. **174**: 2211-2224.

4 **van Pinxteren, L. A., Cassidy, J. P., Smedegaard, B. H., Agger, E. M. and Andersen, P.,** Control of latent Mycobacterium tuberculosis infection is dependent on CD8 T cells. *Eur J Immunol* 2000. **30**: 3689-3698.

5 **Lewinsohn, D. A., Heinzel, A. S., Gardner, J. M., Zhu, L., Alderson, M. R. and Lewinsohn, D. M.,** Mycobacterium tuberculosis-specific CD8+ T cells preferentially recognize heavily infected cells. *Am J Respir Crit Care Med* 2003. **168**: 1346-1352.

6 **Harty, J. T., Tvinnereim, A. R. and White, D. W.,** CD8+ T cell effector mechanisms in resistance to infection. *Annu Rev Immunol* 2000. **18**: 275-308.

7 **Stenger, S., Mazzaccaro, R. J., Uyemura, K., Cho, S., Barnes, P. F., Rosat, J. P., Sette, A.*et al.*,** Differential effects of cytolytic T cell subsets on intracellular infection. *Science* 1997. **276**: 1684-1687.

8 **Woodworth, J. S., Wu, Y. and Behar, S. M.,** Mycobacterium tuberculosis-specific CD8+ T cells require perforin to kill target cells and provide protection in vivo. *J Immunol* 2008. **181**: 8595-8603.

9 **Bruns, H., Meinken, C., Schauenberg, P., Harter, G., Kern, P., Modlin, R. L., Antoni, C.*et al.*,** Anti-TNF immunotherapy reduces CD8+ T cell-mediated antimicrobial activity against Mycobacterium tuberculosis in humans. *J Clin Invest* 2009. **119**: 1167-1177.

10 **Mahnke, Y. D., Brodie, T. M., Sallusto, F., Roederer, M. and Lugli, E.,** The who's who of T-cell differentiation: human memory T-cell subsets. *Eur J Immunol* 2013. **43**: 2797-2809.

11 **Rozot, V., Vigano, S., Mazza-Stalder, J., Idrizi, E., Day, C. L., Perreau, M., Lazor-Blanchet, C.*et al.*,** Mycobacterium tuberculosis-specific CD8+ T cells are functionally and phenotypically different between latent infection and active disease. *Eur J Immunol* 2013. **43**: 1568-1577.

12 **Chiacchio, T., Petruccioli, E., Vanini, V., Cuzzi, G., Pinnetti, C., Sampaolesi, A., Antinori, A.*et al.*,** Polyfunctional T-cells and effector memory phenotype are associated with active TB in HIV-infected patients. *J Infect* 2014.

13 **Ongaya, A., Huante, M. B., Mwangi, P., Keiser, P. H., Amukoye, E. and Endsley, J. J.,** Mycobacterium tuberculosis-specific CD8+ T cell recall in convalescing TB subjects with HIV co-infection. *Tuberculosis (Edinb)* 2013. **93 Suppl**: S60-65.

14 **Bottasso, O., Bay, M. L., Besedovsky, H. and del Rey, A.,** The immuno-endocrine component in the pathogenesis of tuberculosis. *Scand J Immunol* 2007. **66**: 166-175.

15 **Dillon, J. S.,** Dehydroepiandrosterone, dehydroepiandrosterone sulfate and related steroids: their role in inflammatory, allergic and immunological disorders. *Curr Drug Targets Inflamm Allergy* 2005. **4**: 377-385.

16 **Reading, C., Dowding, C., Schramm, B., Garsd, A., Onizuka-Handa, N., Stickney, D. and Frincke, J.,** Improvement in immune parameters and human immunodeficiency virus-1 viral response in individuals treated with 16alpha-bromoepiandrosterone (HE2000). *Clin Microbiol Infect* 2006. **12**: 1082-1088.

17 **Stickney, D. R., Noveljic, Z., Garsd, A., Destiche, D. A. and Frincke, J. M.,** Safety and activity of the immune modulator HE2000 on the incidence of tuberculosis and other opportunistic infections in AIDS patients. *Antimicrob Agents Chemother* 2007. **51**: 2639-2641.

18 **Hernandez-Pando, R., Aguilar-Leon, D., Orozco, H., Serrano, A., Ahlem, C., Trauger, R., Schramm, B.*et al.*,** 16alpha-Bromoepiandrosterone restores T helper cell type 1 activity and accelerates chemotherapy-induced bacterial clearance in a model of progressive pulmonary tuberculosis. *J Infect Dis* 2005. **191**: 299-306.

19 **Quiroga, M. F., Angerami, M. T., Santucci, N., Ameri, D., Francos, J. L., Wallach, J., Sued, O.*et al.*,** Dynamics of adrenal steroids are related to variations in Th1 and Treg populations during Mycobacterium tuberculosis infection in HIV positive persons. *PLoS One* 2012. **7**: e33061.

20 **Hamann, D., Baars, P. A., Rep, M. H., Hooibrink, B., Kerkhof-Garde, S. R., Klein, M. R. and van Lier, R. A.,** Phenotypic and functional separation of memory and effector human CD8+ T cells. *J Exp Med* 1997. **186**: 1407-1418.

21 **Mailloux, A. W., Sugimori, C., Komrokji, R. S., Yang, L., Maciejewski, J. P., Sekeres, M. A., Paquette, R.*et al.*,** Expansion of effector memory regulatory T cells represents a novel prognostic factor in lower risk myelodysplastic syndrome. *J Immunol* 2012. **189**: 3198-3208.

22 **Khamesipour, A., Nateghi Rostami, M., Tasbihi, M., Miramin Mohammadi, A., Shahrestani, T., Sarrafnejad, A., Sohrabi, Y.*et al.*,** Phenotyping of circulating CD8(+) T cell subsets in human cutaneous leishmaniasis. *Microbes Infect* 2012.

23 **Larbi, A. and Fulop, T.,** From "truly naive" to "exhausted senescent" T cells: when markers predict functionality. *Cytometry A* 2014. **85**: 25-35.

24 **Ghiglione, Y., Falivene, J., Ruiz, M. J., Laufer, N., Socias, M. E., Cahn, P., Giavedoni, L.*et al.*,** Early skewed distribution of total and HIV-specific CD8+ T-cell

memory phenotypes during primary HIV infection is related to reduced antiviral activity and faster disease progression. *PLoS One* 2014. **9**: e104235.

25 **Gray, J. M. and Cohn, D. L.,** Tuberculosis and HIV coinfection. *Semin Respir Crit Care Med* 2013. **34**: 32-43.

26 **Helke, K. L., Mankowski, J. L. and Manabe, Y. C.,** Animal models of cavitation in pulmonary tuberculosis. *Tuberculosis (Edinb)* 2006. **86**: 337-348.

27 **Rhee, I. and Veillette, A.,** Protein tyrosine phosphatases in lymphocyte activation and autoimmunity. *Nat Immunol* 2012. **13**: 439-447.

28 **Do, H. T., Baars, W., Borns, K., Windhagen, A. and Schwinzer, R.,** The 77C->G mutation in the human CD45 (PTPRC) gene leads to increased intensity of TCR signaling in T cell lines from healthy individuals and patients with multiple sclerosis. *J Immunol* 2006. **176**: 931-938.

29 **Wang, Y. and Johnson, P.,** Expression of CD45 lacking the catalytic protein tyrosine phosphatase domain modulates Lck phosphorylation and T cell activation. *J Biol Chem* 2005. **280**: 14318-14324.

30 **Breton, G., Chomont, N., Takata, H., Fromentin, R., Ahlers, J., Filali-Mouhim, A., Riou, C.*et al.*,** Programmed death-1 is a marker for abnormal distribution of naive/memory T cell subsets in HIV-1 infection. *J Immunol* 2013. **191**: 2194-2204.

31 **Buggert, M., Tauriainen, J., Yamamoto, T., Frederiksen, J., Ivarsson, M. A., Michaelsson, J., Lund, O.*et al.*,** T-bet and Eomes are differentially linked to the exhausted phenotype of CD8+ T cells in HIV infection. *PLoS Pathog* 2014. **10**: e1004251.

32 **Kaech, S. M. and Cui, W.,** Transcriptional control of effector and memory CD8+ T cell differentiation. *Nat Rev Immunol* 2012. **12**: 749-761.

33 **Behar, S. M.,** Antigen-specific CD8(+) T cells and protective immunity to tuberculosis. *Adv Exp Med Biol* 2013. **783**: 141-163.

34 **Champagne, P., Ogg, G. S., King, A. S., Knabenhans, C., Ellefsen, K., Nobile, M., Appay, V.*et al.*,** Skewed maturation of memory HIV-specific CD8 T lymphocytes. *Nature* 2001. **410**: 106-111.

35 **Wallis, R. S., Kim, P., Cole, S., Hanna, D., Andrade, B. B., Maeurer, M., Schito, M.*et al.*,** Tuberculosis biomarkers discovery: developments, needs, and challenges. *Lancet Infect Dis* 2013. **13**: 362-372.

36 **Shao, L., Zhang, W., Zhang, S., Chen, C. Y., Jiang, W., Xu, Y., Meng, C.*et al.*,** Potent immune responses of Ag-specific Vgamma2Vdelta2+ T cells and CD8+ T cells associated with latent stage of Mycobacterium tuberculosis coinfection in HIV-1-infected humans. *Aids* 2008. **22**: 2241-2250.

37 **Caccamo, N., Meraviglia, S., La Mendola, C., Guggino, G., Dieli, F. and Salerno, A.,** Phenotypical and functional analysis of memory and effector human CD8 T cells specific for mycobacterial antigens. *J Immunol* 2006. **177**: 1780-1785.

38 **Mattila, J. T., Diedrich, C. R., Lin, P. L., Phuah, J. and Flynn, J. L.,** Simian immunodeficiency virus-induced changes in T cell cytokine responses in cynomolgus macaques with latent Mycobacterium tuberculosis infection are associated with timing of reactivation. *J Immunol* 2011. **186**: 3527-3537.

39 **Zhou, F.,** Molecular mechanisms of IFN-gamma to up-regulate MHC class I antigen processing and presentation. *Int Rev Immunol* 2009. **28**: 239-260.

40 **Woodworth, J. S. and Behar, S. M.,** Mycobacterium tuberculosis-specific CD8+ T cells and their role in immunity. *Crit Rev Immunol* 2006. **26**: 317-352.

41 **Angerami, M., Suarez, G., Pascutti, M. F., Salomon, H., Bottasso, O. and Quiroga, M. F.,** Modulation of the phenotype and function of Mycobacterium tuberculosis-stimulated dendritic cells by adrenal steroids. *Int Immunol* 2013. **25**: 405-411.

42 **Takemoto, N., Intlekofer, A. M., Northrup, J. T., Wherry, E. J. and Reiner, S. L.,** Cutting Edge: IL-12 inversely regulates T-bet and eomesodermin expression during pathogen-induced CD8+ T cell differentiation. *J Immunol* 2006. **177**: 7515-7519.

43 **OARAC,** Panel on Antiretroviral Guidelines for Adults and Adolescents. Guidelines for the use of antiretroviral agents in HIV-1-infected adults and adolescents. In **http://www.aidsinfo.nih.gov/ContentFiles/AdultandAdolescentGL.pdf** (Ed.) 2011.

44 **Quiroga, M. F., Pasquinelli, V., Martinez, G. J., Jurado, J. O., Zorrilla, L. C., Musella, R. M., Abbate, E.*et al.*,** Inducible costimulator: a modulator of IFN-gamma production in human tuberculosis. *J Immunol* 2006. **176**: 5965-5974.

45 **Quiroga, M. F., Jurado, J. O., Martinez, G. J., Pasquinelli, V., Musella, R. M., Abbate, E., Issekutz, A. C.*et al.*,** Cross-talk between CD31 and the signaling lymphocytic activation molecule-associated protein during interferon- gamma production against Mycobacterium tuberculosis. *J Infect Dis* 2007. **196**: 1369-1378.

46 **Betts, M. R., Brenchley, J. M., Price, D. A., De Rosa, S. C., Douek, D. C., Roederer, M. and Koup, R. A.,** Sensitive and viable identification of antigen-specific CD8+ T cells by a flow cytometric assay for degranulation. *J Immunol Methods* 2003. **281**: 65-78.

47 **Ruijter, J. M., Ramakers, C., Hoogaars, W. M., Karlen, Y., Bakker, O., van den Hoff, M. J. and Moorman, A. F.,** Amplification efficiency: linking baseline and bias in the analysis of quantitative PCR data. *Nucleic Acids Res* 2009. **37**: e45.

48 **Roederer, M., Nozzi, J. L. and Nason, M. C.,** SPICE: exploration and analysis of post-cytometric complex multivariate datasets. *Cytometry A* 2011. **79**: 167-174.

Figure 1. *Effector/memory phenotype and transitions in total peripheral CD8+T cells from HIV-TB, HIV$^+$, HIV-LTB and HD.* Recently thawed or freshly isolated PBMCs were stained for the expression of CD45RA and CD27 in CD8$^+$T cells as described in *Methods*. (A -E) The expression of CD27 and CD45RA on CD8$^+$T cells from HD, HIV$^+$, HIV-LTB and HIV-TB patients was analysed by flow cytometry; (A) (top) Pie charts summarize the data and each slice corresponds to the mean proportion of CD8$^+$T cells for each phenotype. (Bottom) Possible phenotypes are shown on the x-axis whereas percentages of distinct T-cell subsets within CD8$^+$T cells are shown on the y-axis. Comparisons of phenotype distribution were performed using the partial permutation test as described in [48] and the Kruskall-Wallis test followed by Dunn's multiple comparisons post-test. (B) Representative flow cytometry dot plot examples from an HD (top) and an HIV-TB patient (bottom). CD8$^+$T cells were gated as shown in Supporting information Fig. 1. (C) T_{TE}/T_{EM} ratio for each individual is shown. Comparisons were performed by the Kruskall-Wallis test followed by Dunn's multiple comparisons post-test. (D) Correlation analysis between the % of Terminal Effectors (T_{TE}) and the % of Effector Memory (T_{EM}) in CD8$^+$T cells were evaluated to assess recent effector/memory transitions as described previously [21, 24]. Figure shows % of T_{TE} vs. % of T_{EM} in 27 HIV-TB (left) and 14 HD (right) subjects. Continuous lines represent linear regression curves and dashed lines represent 95% confidence intervals. Sp. r: Spearman's rank correlation coefficient. (E) Cumulative analyses of the expression of CD27 and CD45RA on CD8$^+$T cells from HIV-TB subjects stratified according to TB presentation (left), smear status (middle) and highly active antiretroviral therapy (HAART, right). Possible phenotypes are shown on the x-axis whereas percentages of distinct T-cell subsets within CD8$^+$T cells are shown on the y-axis. Comparisons of phenotype distribution were performed using the partial permutation test as described in [48] and the Kruskall-Wallis test followed by Dunn's multiple comparisons post-test. (A-E) Each symbol represents an individual subject (n values are shown in the figure). Horizontal lines represent median values and boxes represent interquartile range. * $p<0.05$; ** $p<0.01$; ***$p<0.001$.

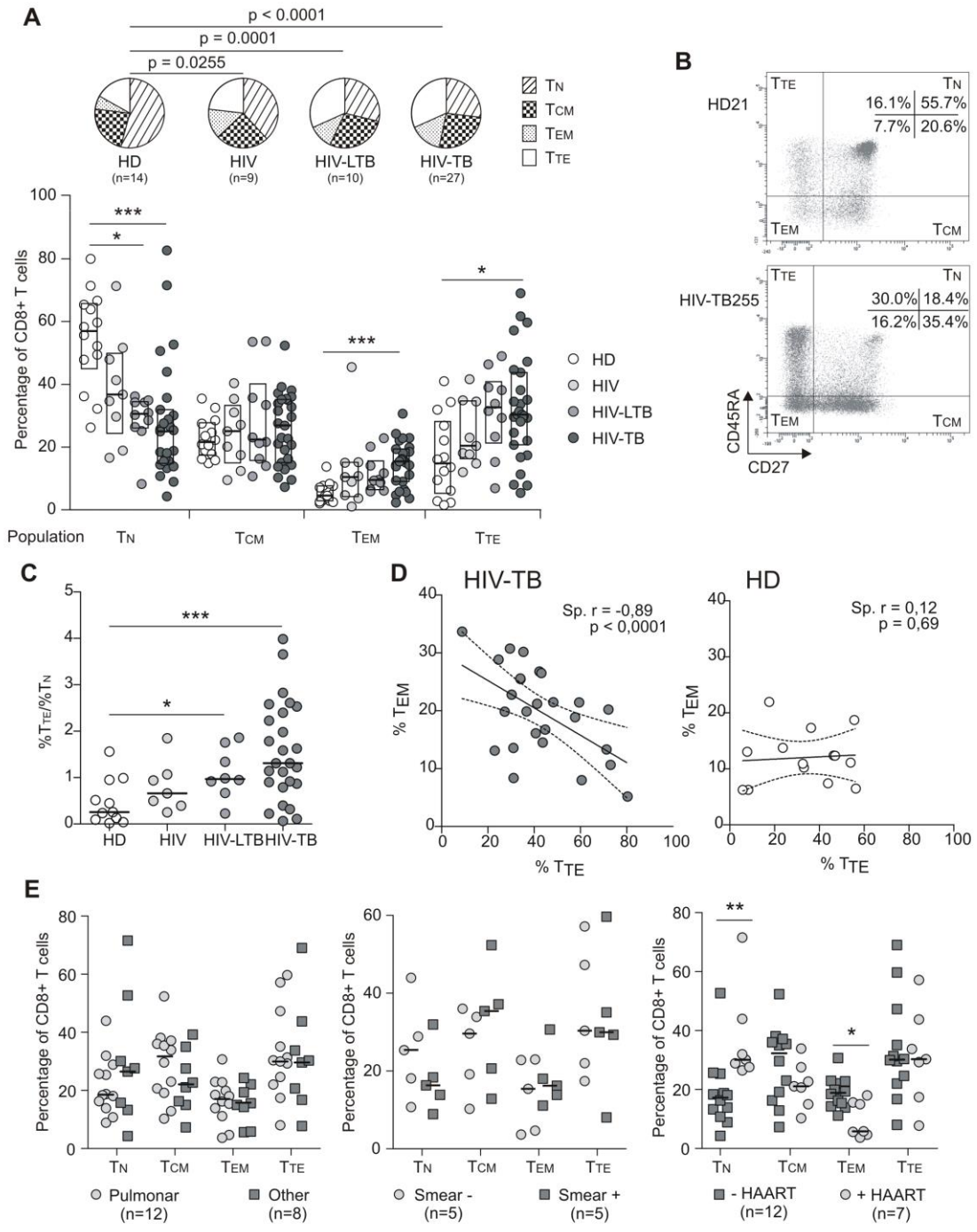

Figure 2. *Phenotype of terminally differentiated CD8$^+$T cells in HIV-TB, HIV$^+$, HIV-LTB and HD.* Recently thawed or freshly isolated PBMCs were stained for CD27, CD45RA and PD1 as described in *Methods* and analyzed by flow cytometry. (A) Analysis of the relative mean fluorescence intensity (MFI) of CD45RA in T_{TE} CD8$^+$T cells as defined by the ratio: [CD45RA MFI on T_{TE} / CD45RA MFI on T_N]. Horizontal lines represent median values, boxes represent interquartile ranges and whiskers represent 95% confidence intervals. (B, C) % of CD45RA^{dim} T_{TE} and CD45RA^{hi} T_{TE} among CD8$^+$T cells defined as described in Supporting Information Fig. 1. (C) Representative flow cytometry histogram examples showing the expression of CD45RA in CD27^{neg} CD8$^+$T cells from an HD (filled curve) and an HIV-TB patient (open curve). (D) % of PD1$^+$ (left) and CD27^{neg} (right) cells among CD8$^+$T cells from HD (n=15), HIV$^+$ (n=8), HIV-LTB (n=10) and HIV-TB (n=24) subjects was determined by flow cytometry. (E) (left) Representative dot plots for the expression of CD27 vs. PD1 in total CD8$^+$T cells from an HIV-TB and an HD subject and cumulative analysis of PD1 expression in CD27^{neg} and CD27$^+$ CD8$^+$T cells from HIV-TB and HD (right). Each line connects the data for an individual patient. Comparisons between the CD27$^+$ and CD27^{neg} populations were performed using the Wilcoxon matched pairs test. (F) Correlation analysis between the % of CD45RA^{dim} T_{TE} CD8$^+$ cells and % of PD1 in CD27$^+$/CD8$^+$ cells in 23 HIV-TB patients. Continuous lines represent linear regression curves and dashed lines represent 95% confidence intervals. Sp. r: Spearman's rank coefficient. (B and D) Comparisons between groups were evaluated by the Kruskall-Wallis test followed by Dunn's multiple comparisons post-test. Horizontal lines represent median values, boxes represent interquartile ranges and whiskers represent 95% confidence intervals. Each symbol represents an individual subject. N values are shown in the figure. * $p<0.05$; ** $p<0.01$; ***$p<0.001$.

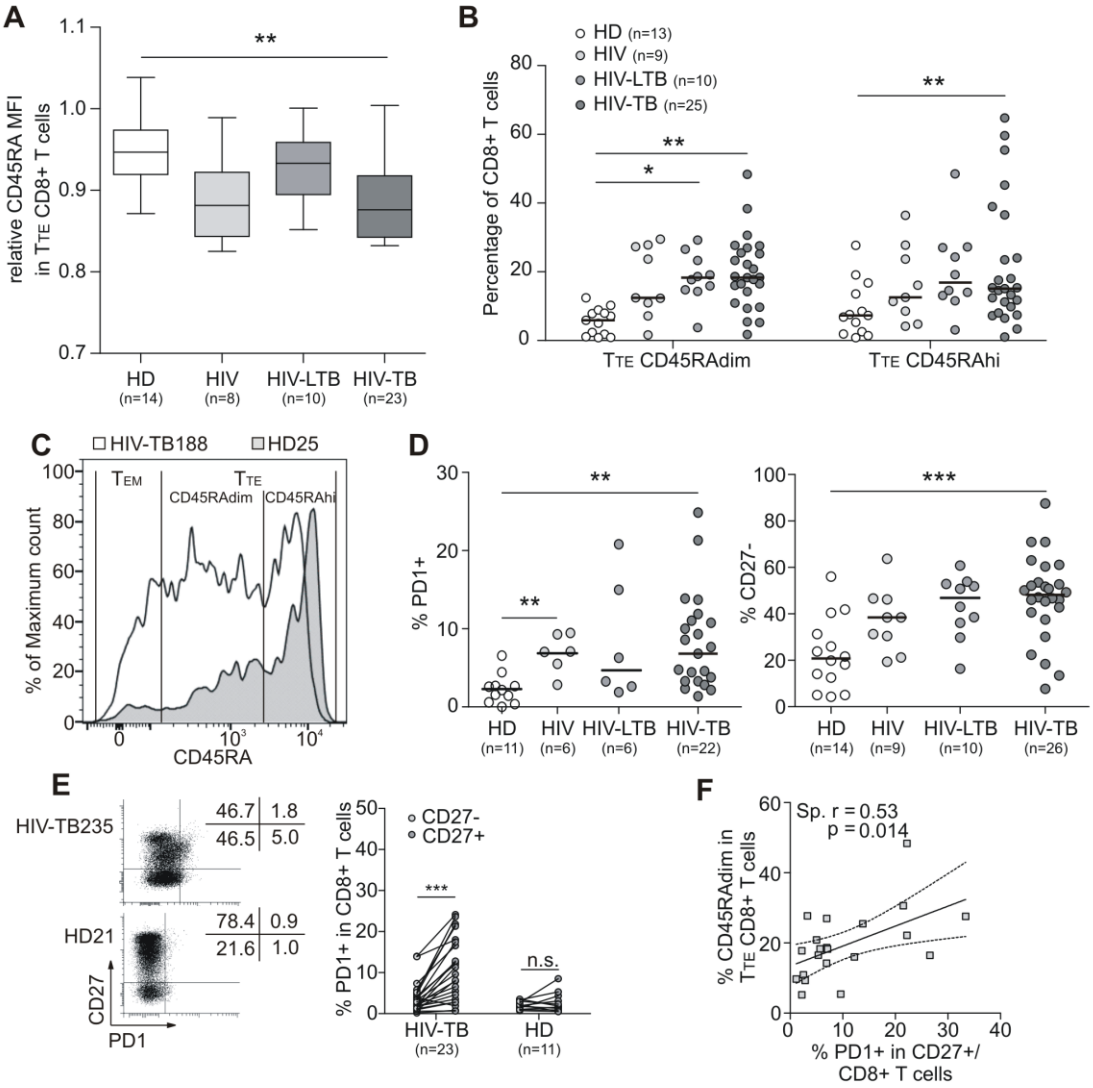

Figure 3. *Effector/memory phenotype and transitions in* Mtb-*specific CD8$^+$T cells from HIV-TB patients and HD*. (A) CD8$^+$T cells from HD, HIV, HIV-LTB and HIV-TB individuals were in vitro stimulated and analyzed after 16 h for *Mtb*-induced CD107a/b and IFN-γ expression by flow cytometry. Comparisons between groups were performed using the Kruskall-Wallis test followed by Dunn's multiple comparisons post-test. (B-D) CD8$^+$T cells from HD and HIV-TB individuals were in vitro stimulated and analysed after 72 h for *Mtb*-induced CD107a/b, IFN-γ, CD27 and CD45RA expression by flow cytometry. CD8$^+$T cells were gated as shown in Supplementary Information Fig. 1. The gating strategy is based on the distribution of CD27 and CD45RA on bulk CD8$^+$ T cells and it is then conserved in the analyses of CD107a/b$^+$ or IFN-γ^+ CD8$^+$ T cells. (B) Representative dot plots of the expression of CD107a/b$^+$ vs. CD8 in CD8$^+$T cells (left), CD27 vs. CD45RA in CD107a/b$^+$ CD8$^+$T cells (middle) and CD27 vs. CD45RA in bulk CD8$^+$T cells (right) from an HD (top) and an HIV-TB patient (bottom). (C) Expression of CD27 and CD45RA on *Mtb*-specific CD8$^+$T cells from HD and HIV-TB individuals. (Left) Pie charts summarize the data and each slice corresponds to the mean proportion of *Mtb*-specific CD8$^+$T cells of each phenotype. (Right) Possible phenotypes are shown on the x-axis whereas percentages of distinct T-cell subsets within *Mtb*-specific CD8$^+$ T cells are shown on the y-axis. Comparisons of phenotype distribution were performed using the partial permutation test and the Kruskall-Wallis test followed by Dunn's multiple comparisons post-test. (D) Correlation analysis between the % of T_{TE} and the % of T_N, T_{CM} or T_{EM} in CD107a/b$^+$ and IFN-γ^+ CD8$^+$T cells were evaluated in HIV-TB (white background) and HD (grey background) subjects. Continuous lines represent linear regression curves and dashed lines represent 95% confidence intervals. Sp. r: Spearman's rank coefficient. (A-D) Horizontal lines represent median values and boxes represent interquartile range. Each symbol represents an individual subject. N values are shown in the figure. * $p<0.05$; ** $p<0.01$; ***$p<0.001$.

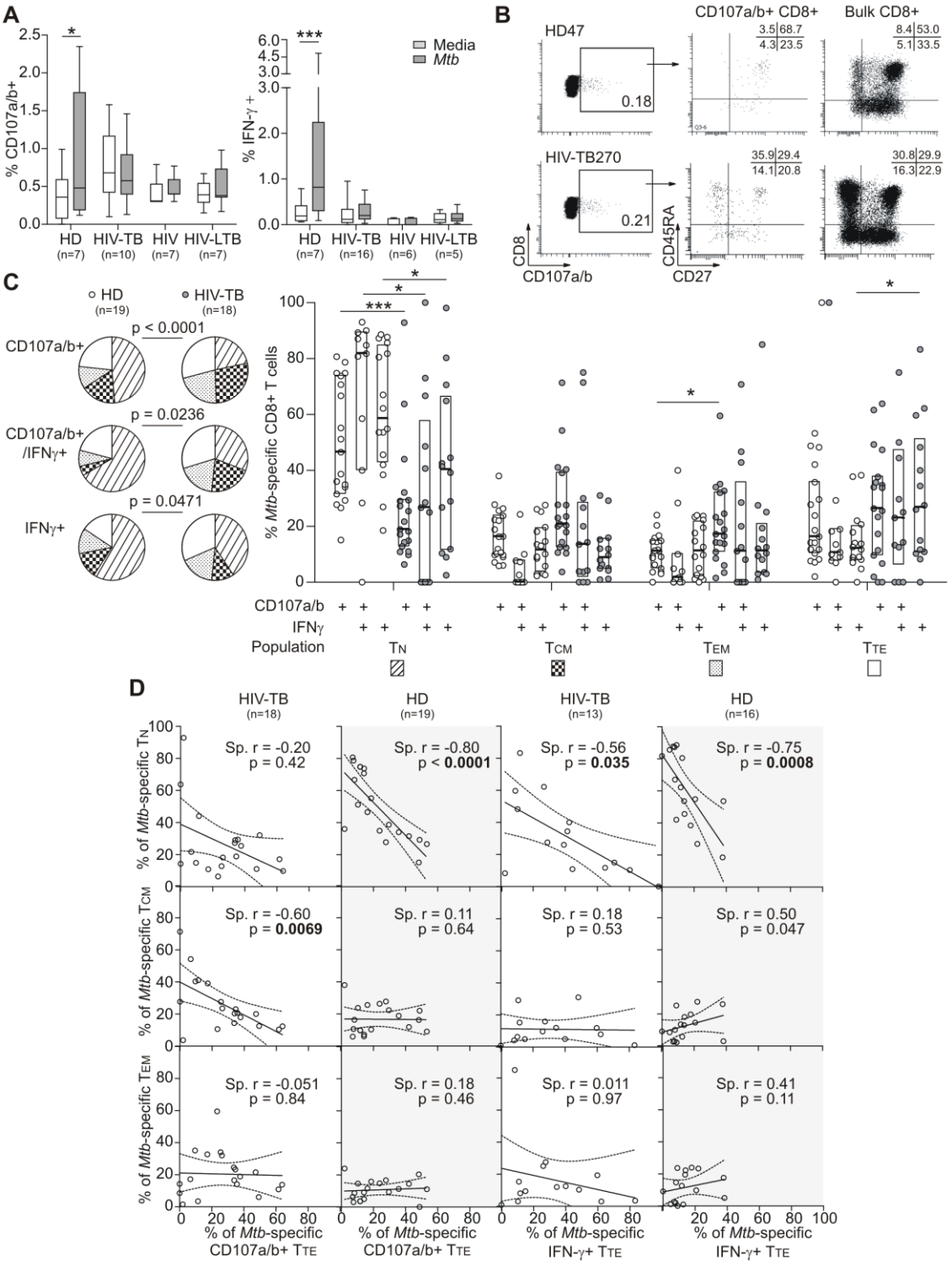

Figure 4. *Adrenal hormone levels and their association with CD8$^+$T cells differentiation and function.* (A) Recently thawed PBMCs were stained for the expression of CD45RA and CD27 and analysed by flow cytometry. Plasma levels of DHEA were measured in the same blood samples as described in *Methods*. Figure shows correlation analyses between (top) the % of T_{TE} or (bottom) T_{TE} CD45RA^{hi} in CD8$^+$T cells and dehydroepiandrosterone (DHEA) plasma levels in (left) HIV$^+$, (middle) HIV-LTB and (right) HIV-TB subjects. (B) PBMCs were incubated in the presence or absence of *Mtb* or HIV peptides and then the expression of CD107a/b, CD45RA and CD27 were analyzed by flow cytometry. Plasma levels of cortisol were measured in the same blood samples as described in *Methods.* Figure shows correlation analysis between cortisol plasma levels and the % of *Mtb*-specific CD107a/b$^+$ CD8$^+$T cells in (left) HIV-TB and (middle) HD subjects or (right) the % of HIV-specific CD107a/b$^+$ CD8$^+$T cells in chronic HIV$^+$ subjects. (A, B) Values were media-subtracted and negative values were set to zero. Continuous lines represent linear regression curves and dashed lines represent 95% confidence intervals. Sp. r: Spearman's rank coefficient. Each symbol represents an individual subject. (C) PBMCs were incubated in the presence or absence of *Mtb* with or without DHEA and then the expression of CD107a/b and IFN-γ was evaluated in CD8$^+$T cells from 11 HIV-TB patients with CD4$^+$ T-cell counts higher than 100 cells/μl. Values were media-subtracted and negative values were set to zero. Each line connects the data for an individual patient. Comparisons between treatments were performed using the Wilcoxon matched pairs test. * p<0.05.

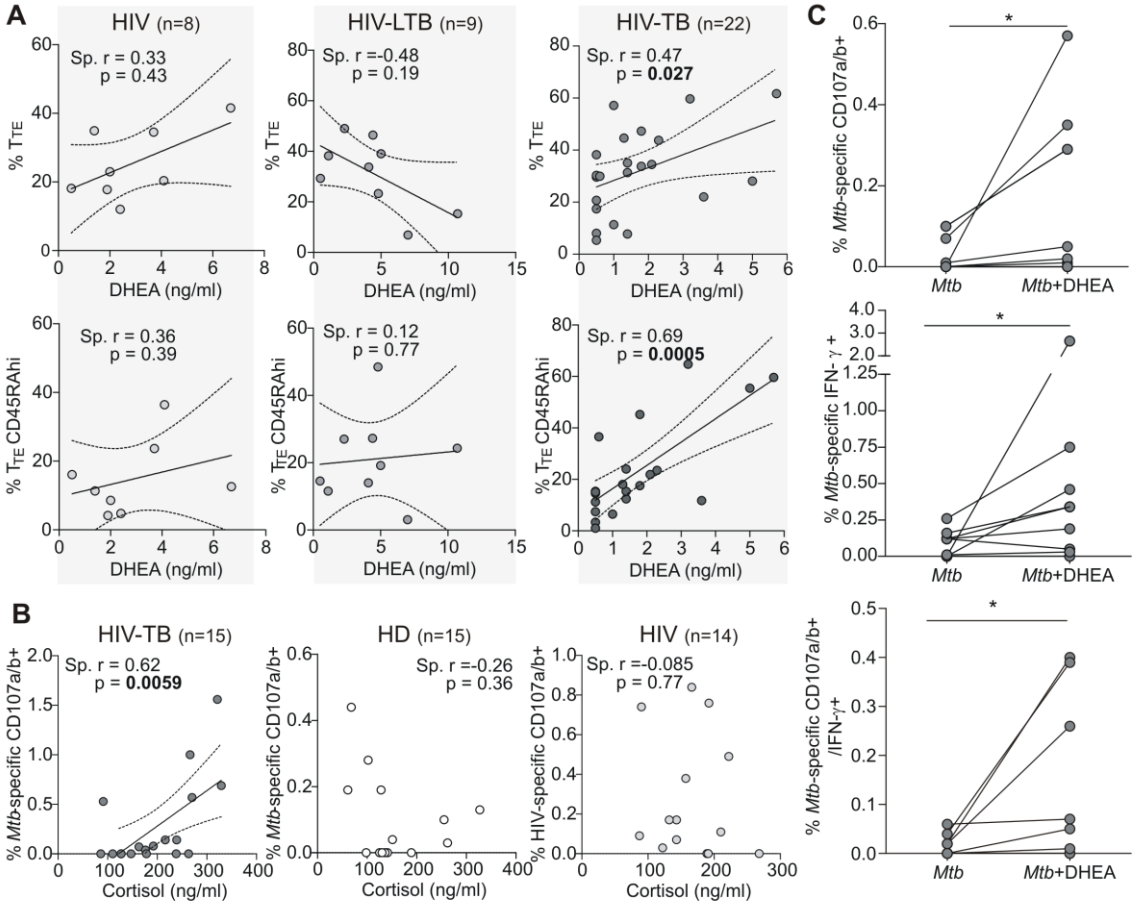

Figure 5. *DHEA effect on Mtb-specific responses and terminal differentiation in CD8$^+$T cells from HIV-TB patients.* (A-B) PBMCs from HIV-TB patients were stimulated with *Mtb* or *Mtb* supplemented with DHEA for 72 h and CD107a/b, IFN-γ, CD27 and CD45RA expression was analyzed by flow cytometry. (A) (Left) Frequencies of CD107a/b$^+$ (n=17), (middle) IFN-γ^+ (n=11) or (right) bifunctional CD107a/b$^+$/IFN-γ^+ (n=13) T_N, T_{EM}, T_{CM} and T_{TE} cells among CD8$^+$T cells from HIV-TB patients under basal conditions or after stimulation with *Mtb* or *Mtb* supplemented with DHEA. Bars represent the median value for each phenotype. * $p<0.05$ for % CD107$^+$ T_{TE} cells in CD8$^+$T cells, # $p<0.05$ for % CD107$^+$ cells in CD8$^+$T cells. (B) Representative dot plots showing the expression of CD107a/b vs. FSC among T_{TE} CD8$^+$T cells from a representative HIV-TB patient in basal conditions (Media) or after stimulation with *Mtb* or *Mtb* + DHEA. (C-H) PBMCs from HD subjects were stimulated with *Mtb* or *Mtb* supplemented with DHEA for 72 h. Then, CD8$^+$ cells were isolated by positive selection and mRNA expression of the indicated molecules and GAPDH were determined by real time PCR. Figures show the relative expression to GAPDH of (C) Tbx-21 (Tbet), (D) Eomes, (F) Blimp-1 (G) BCL-6 mRNAs and (E) Tbet/Eomes or (H) Blimp-1/BCL-6 mRNA ratios in isolated CD8$^+$ cells from HD under basal conditions or after stimulation with *Mtb* or *Mtb* supplemented with DHEA. Horizontal lines represent median values, boxes represent interquartile ranges and whiskers represent 95% confidence intervals of 7 donors from 3 independent experiments. (A-G) Comparisons between treatments were performed using the Kruskall-Wallis test followed by Dunns multiple comparisons post-test. * $p<0.05$, ** $p<0.01$.

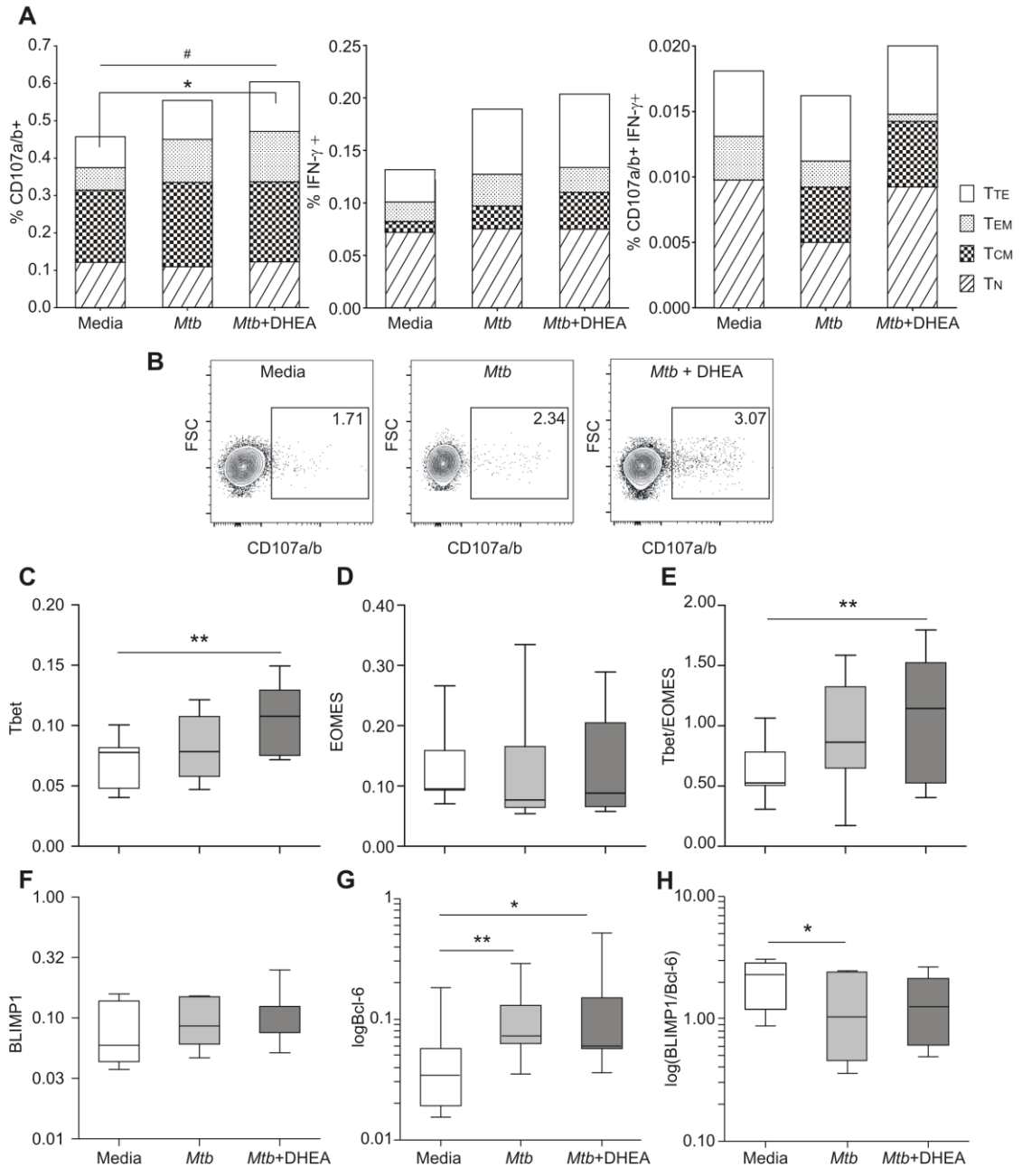

Figure 6. *Correlation analysis between lytic degranulation and IFN-γ production in CD8⁺T cells from HIV-TB patients.* PBMCs from HD or HIV-TB patients were incubated under basal conditions or in the presence of *Mtb, Mtb* supplemented with DHEA or Cytomegalovirus, Epstein-Barr, and Influenza virus control peptide pool (CEF) and then the expression of CD107a/b and IFN-γ in $CD8^+$T cells was evaluated by flow cytometry. Figures show the correlation analyses between the % of $CD107a/b^+$ and the % of $IFN\text{-}\gamma^+$ cells among $CD8^+$T cells from HIV-TB subjects stimulated with (A) *Mtb* (n=31), (B) *Mtb*+DHEA (n=30) or (C) CEF (n=20) and (D) among $CD8^+$T cells from HD subjects stimulated with *Mtb* (n=29). Values were media-subtracted and negative values were set to zero. Each point represents an individual subject. Continuous lines represent linear regression curves and dashed lines represent 5-95% confidence intervals. Sp r: Spearman's rank coefficient.

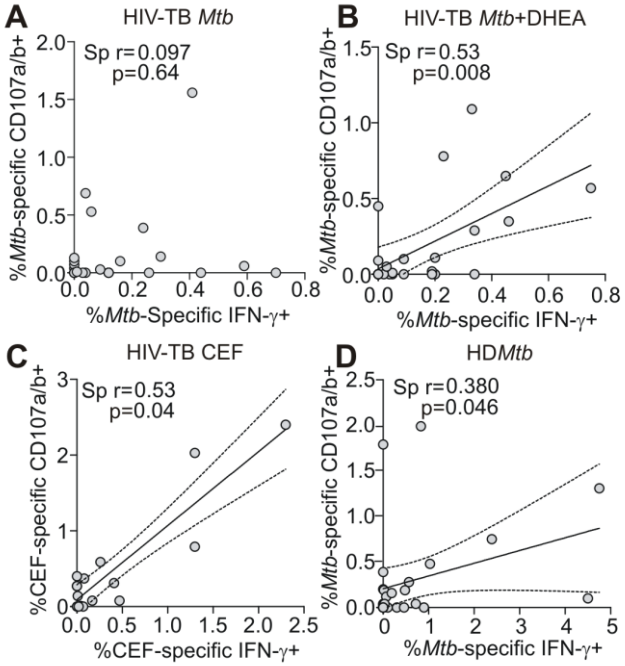

Table 1. Epidemiological characteristics of the subjects enrolled.

	HIV-TB	HIV-LTB	HIV	HD
Number of subjects enrolled	47	11	12	25
Median age in years (IQR)	38 (31-43)	35 (28-40)	35 (32-48)	36 (30-46)
Female/male distribution	21/26	3/8	3/9	16/9
HIV status	+	+	+	-
Median CD4 count (IQR)	93 (37-213)	361 (261-650)	286 (141-452)	843 (607-1075)
Median Viral Load (IQR)	39867 (3789-160732)	12934 (756-24590)	11225 (25-36581)	-

IQR, Interquartile range.